

Pulse Decomposition Analysis of the Digital Arterial Pulse during Hemorrhage Simulation

Martin C. Baruch, PhD **, Darren E. R. Warburton, PhD*, Shannon S. D. Bredin, PhD*, Anita Cote*, David W. Gerdt, PhD **, Charles M. Adkins, PhD **

Abstract—Markers of temporal changes in central blood volume are required to non-invasively detect hemorrhage and the onset of hemorrhagic shock. Recent work suggests that pulse pressure may be such a marker. A new approach to tracking blood pressure, and pulse pressure specifically is presented that is based on a new form of pulse pressure wave analysis called Pulse Decomposition Analysis (PDA). The premise of the PDA model is that the peripheral arterial pressure pulse is a superposition of exactly five individual component pressure pulses, the first of which is due to the left ventricular ejection from the heart while the remaining component pressure pulses are reflections and re-reflections that originate from only two reflection sites within the central arteries. The hypothesis examined here is that the PDA parameter T13, the timing delay between the first and third component pulses, correlates with pulse pressure. T13 was monitored along with blood pressure, as determined by an automatic cuff and another continuous blood pressure monitor, during the course of lower body negative pressure (LBNP) sessions in fifteen subjects. Statistically significant correlations between T13 and pulse pressure were established. The agreement of observations and measurements provides a preliminary validation of a new physical model of the origin and composition of the arterial pressure pulse.

Index Terms—hemorrhage, arterial pulse pressure, pulse reflections, negative lower body pressure

I. INTRODUCTION

THE ability to detect the onset of hemorrhagic shock is of major concern because it remains one of the leading causes of death on the battlefield as well as in civilian trauma cases while also being highly preventable if intervention can be implemented.^{1,2} Mortalities on the battlefield due to

This work was supported by the Office of Naval Research and the National Institutes of Health for portions of this research through contract N00014-09-M-0146 and grant 1R43HL087476-01A1. M.C. Baruch is with Empirical Technologies Corporation, Charlottesville, VA, USA (phone: 434 296-7000; fax: 434 975-0080; e-mail: mcbaruch2@aim.com).

M.C. Baruch is with Empirical Technologies Corporation (e-mail: mcbaruch2@aim.com).

D.E.R. Warburton is with Cardiovascular Physiology Laboratory, University of British Columbia, Vancouver, British Columbia, Canada

S.S.D. Bredin is with Cardiovascular Physiology Laboratory, University of British Columbia, Vancouver, British Columbia, Canada

A. Cote is with Cardiovascular Physiology Laboratory, University of British Columbia, Vancouver, British Columbia, Canada.

D.W. Gerdt is with Empirical Technologies Corporation (e-mail: davidetc@firstva.com).

C.A. Adkins is with Empirical Technologies Corporation (e-mail: cadkins4598@embarqmail.com).

hemorrhaging account for about 50% of deaths and traumatic injury hemorrhaging is the leading cause of death for persons under 45, with 40% mortality before a hospital is reached in civilian settings.

In order to detect hemorrhage, markers of temporal changes in central blood volume are required. Recent work suggests that pulse pressure is a sensitive as well as specific marker for central blood loss.^{3,4} However, detecting progressive hemorrhage requires resolution of changes on the order of a few mmHg in pulse pressures of, normally, 35-50 mmHg. Given the separate and unequal uncertainties in determining systole and diastole, using the best brachial cuffs,⁵ such determinations are by and large out of reach even in controlled environments

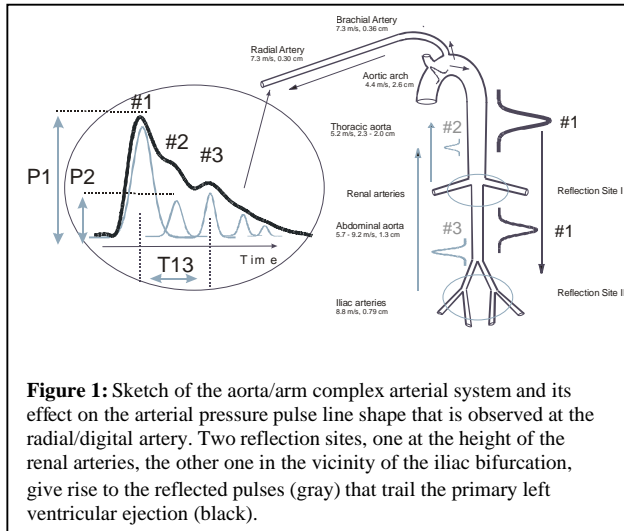
We present here a new approach to tracking blood pressure, and pulse pressure specifically. It is based on a new form of pulse pressure wave analysis, implemented through what we refer to as the Pulse Decomposition Analysis (PDA) algorithm.

In view of the different approaches to the contour analysis of the arterial pressure pulse at the radial or digital arteries that have been developed,^{6,7,8,9,10,11} it is reasonable to ask why another one is proposed here. The response is that the current view, as it relates to the origin and the dynamic behavior of the pressure pulse reflections, is not adequate.

A summary of the current view is one where the arterial pulse contour, obtained at the radial or a digital artery, can be divided into two traveling pressure wave parts, a forward traveling wave that emanated from the left ventricle, and a reflected wave traveling in the opposite direction.¹² According to this view, the reflected wave is a summation of different waves that were reflected at various different reflection sites which are “more of a statistical notion than a physically discrete site”.¹³ Among this collection of reflection sites are branching points, changes in arterial wall elasticity, as well as the artery/arteriole interfaces in the arterial periphery. The reason for invoking these interfaces and conditions is that they represent significant impedance mismatches to the forward traveling pressure wave due to the down-step in arterial blood pressure, typically on the order of tens of mmHg.⁸ Interestingly, while some of the reflections are hypothesized to be coming from as far away as the lower body, other authors have raised the possibility of reflections coming from the central arteries,¹² but this dichotomy has not been further explored. Others yet have raised the possibility that the “reflected wave” may in fact have distinct components, as

opposed to being strictly the summation of different wave components. Specifically, according to ORourke, the peripheral “second systolic” peak rises and falls with aortic systolic pressure, at least in hypertensive subjects.¹⁴

We believe that the current view of the source of arterial pressure pulse reflections is only partly true and that the arterial



peripheral pressure pulse is explained succinctly and entirely by considering only two distinct reflection sites that are located in the central arteries. The distinct structure of the arterial pulse follows from several observations. 1. The arterial pressure pulse demonstrates distinct features that have the same temporal characteristics as the primary “wave” that corresponds to the left ventricular ejection, and these features can be manipulated by maneuvers that affect distinct sections of the arterial tree, such as Valsalva. 2. The timing of the reflected wave relative to the primary wave is incompatible with the concept of it having originated in the distant arterial periphery because the arterial pathways to reach the radial or digital palpation site are too long to match the observed time intervals between primary and reflected wave given known arterial pulse propagation velocities.

Instead we propose the physical PDA model of the arterial pressure pulse that is qualitatively summarized in Figure 1. It models the brachial/radial/digital arterial pulse as a superposition of five component pulses, the first of which is the primary pressure pulse due to the left ventricular ejection while the trailing pulses are reflections of the first pulse that originate from two sites within the central arteries. Specifically, we hypothesize that the structure of the peripheral pulse can be explained entirely by the interaction of the primary left ventricular ejection pressure pulse with these two aortic reflection sites. The first reflection site is the juncture between thoracic and abdominal aorta, which is marked by a significant decrease in diameter and a change in elasticity and the second site arises from the juncture between abdominal aorta and iliac arteries. The first reflection site is located approximately at the height of the renal arteries and gives rise to the peak labeled #2 in Figure 1. It is important to note that it is the change in aortic diameter and elasticity that gives rise to the #2 reflected pulse,

and not the presence of the small renal arteries. The #2 pulse is commonly known as the “second systolic” peak. We refer to it as the “renal reflection” and it follows the primary ejection pulse (#1) into the arterial periphery of the arm at delays of between 70-140 milliseconds.

The second central artery reflection site gives rise to the much larger “iliac reflection”, labeled #3 in Figure 1, which follows the #1 pulse at delays of 180 to 400 milliseconds. Additional reflected pulses, due to re-reflections, follow the two initial ones, but are less relevant for quantitative analysis due to their poorer signal to noise characteristics and the fact that they are easily swallowed by the pulse envelope of the next cardiac cycle unless the heart rate is very low.

The PDA model presented here analyzes the arterial pulse as observed on the lower arm by isolating, identifying and quantifying the temporal positions and amplitudes of the renal reflection (#2) and the iliac reflection (#3) each relative to the primary systolic peak (#1), within the pulse shape envelope of an individual cardiac cycle. The model’s predictions and experimental studies show that two pulse parameters are of particular importance. One parameter is the ratio of the amplitude of the renal reflection (#2) to that of the primary systolic peak (#1). These amplitudes, labeled P1 and P2, are indicated in to the left of the arterial pressure pulse envelope. This parameter is herein referred to as the P2P1 ratio and it tracks changes in central beat-by-beat systolic pressure. The second parameter is the time difference between the arrival of the primary systolic (#1) pulse and the iliac reflection (#3) pulse. This parameter is referred to as T13, as indicated in Figure 1, and it tracks changes in arterial pulse pressure, also beat-by-beat.

It is the aim of this paper to validate the described arterial pressure pulse reflection scenario through the presentation of experimental data collected in the context of simulating central hemorrhage and its comparison with predictions of the PDA pulse propagation model. Specifically, our hypothesis is that the time delay between the primary component pulse (#1) and the iliac reflection pulse (#3), T13, correlates with pulse pressure

We report here the results of monitoring the evolution of the PDA parameter T13 during the course of lower body negative pressure (LBNP) sessions. LBNP is an established technique used to physiologically stress the cardiovascular system. It has been used to simulate gravitational stress and hemorrhage, alter preload, and to manipulate baroreceptors.¹⁵ LBNP was chosen for this project because it has been shown to be very effective at modulating pulse pressure, thereby providing a means to validate the equivalent PDA arterial pulse parameter, T13.

II. PATIENTS AND METHODS

After IRB approval, tests of the CareTaker™ system, which is the hardware implementation of the PDA model that is described in more detail below, were performed at the Cardiovascular Physiology Laboratory of the University of British Columbia on fifteen healthy volunteers (average age: 24.4 years, SD: 3.0

years; average height: 168.6 cm, SD: 8.0 cm; average weight: 64.0 kg, SD: 9.1 kg) whose lower bodies, from the height of the iliac crest downwards, were subjected to increasingly negative pressures. A number of studies have demonstrated that it is possible to simulate significant internal hemorrhage using LBNP. Negative pressures of 10-20 mmHg correspond to 400 to 550 ml of central blood loss, 20-40 mmHg correspond to 500 to 1000 ml, and negative pressures in excess of -40 mmHg correspond to blood losses exceeding 1000 ml.¹⁶

The subjects were subjected to four stages of negative pressure, -15 mmHg, -30 mmHg, -45 mmHg, and -60 mmHg, each stage lasting typically about 12 minutes. The blood pressure was monitored with an automatic cuff (BP TRU Automated Non-Invasive Blood Pressure Monitor (model BPM-100), VSM MedTech Devices Inc.) set to record blood pressures every three minutes, resulting in typically four readings per LBNP setting as well as an Ohmeda 2300 Finapres, and a pulse oximeter (Ohmeda Biox 3740 Pulse Oximeter, BOC Health Care) monitored oxygen saturation. The CareTaker system collected arterial pulse shapes via a finger cuff attached to the central phalange of the middle digit. Four subjects became presyncopal and could not complete the -60 mmHg LBNP stage.

A. CareTaker Device

The hardware platform that provides the arterial pulse signal for the PDA algorithm's analysis is the CareTaker™ device (Empirical Technologies Corporation, Charlottesville, Virginia). It is a physiological sensing system whose three basic physical components are a sensing pad such as a finger cuff that couples to arterial pressure point, such as the middle phalange of the middle digit, a pressure line that pneumatically telemeters the pulsations, and a custom-designed piezo-electric pressure sensor that converts the pressure pulsations, using transimpedance amplification, into a voltage signal that can be measured, digitized, transmitted and recorded. The coupling to the artery is accomplished using palpation coupling, such as at the radial artery, or approximate hydrostatic coupling, such as at the digital arteries. The completely self-contained device wirelessly transmits its signal representing the arterial pulse to a PC computer using the Bluetooth protocol. The device is not occlusive as it operates at a coupling pressure of about 40 mmHg. Another important characteristic of the device is that the signal it provides, sampled at 512 Hz, is the *time derivative* of the arterial pulse signal. The derivative provides significant signal to noise advantage and lowers the resolution requirements for digital acquisition of the signal because the derivative eliminates signal offsets. That is, the signal is always clamped to the signal base line, which in turn allows for increased amplification.

B. Pulse Decomposition Algorithm (PDA)

The basic components of the algorithm are 1. a peak finder that identifies heartbeats in the derivative data stream, 2. a

differentiator that produces the second derivative of the detected heart beat which is then used to find the inversions corresponding to the locations of the component pulses, 3. a digital integrator, implemented as a Bessel filter, that generates the integrated pulse wave form from the differentiated raw signal stream, and from which relative component pulse amplitudes are determined and 4. a low-pass filter that allows identification of the primary systolic peak. Furthermore the frequency content of the data stream is continuously analyzed in order to calculate signal to noise (S/N) figures of merit that determine whether signal fidelity is sufficiently high to permit peak detection and analysis.

Once the temporal locations of the reflection component pulses and the systolic peak are identified, the T13 interval, the time delay between systolic (P1) and iliac peak (P3), is calculated. The P2P1 ratio is calculated using the amplitudes of the P2 peak and the systolic peak, in the integrated pulse spectrum.

C. Statistical Analysis

We present regression coefficients between LBNP levels and pulse pressure responses of the three measurement systems. In order to compare relative sensitivities of the three systems to changes in pulse pressure we present results of different repeated measures ANOVA analyses, which were performed using the Minitab statistical software (Release 14, Minitab Ltd.). Data are presented as means \pm SE unless specified otherwise.

III. RESULTS

A. Comparison of Pulse Pressure Changes

In Figure 2 we present an example of the evolution of arterial pressure pulse line shape changes for the 6 stages of an hour-long LBNP session (right-hand graph B) as well as the T13 trace for the entire session (left graph A). The subject in this case was a 31 y. female. The time evolution of the presented pulse line shapes is downward, starting at the top at atmospheric pressure, and ending with a pulse line shape obtained after the LBNP chamber was vented from -60 mmHg back to atmospheric pressure. Each pulse line shape represents a 10-pulse average.

The dynamic range of the iliac and renal peak positions is indicated by the downward sweeping arrows, while the position of the primary systolic peak (#1) is indicated by the vertical solid arrow. The narrowing of the time interval between iliac and systolic component pulses with decreasing negative pressure is clearly visible. Furthermore, while the heart rate also changed, as indicated by the shortening inter-beat interval, it is clear that the *rates of change* for T13 and heart rate are different, i.e. the inter-beat interval narrowed faster than T13. A further point of interest is the shape of the arterial pressure pulse after venting, which in all subjects caused a significant rise in systolic blood pressure, as determined using the conventional blood pressure monitors. The pressure pulse line shape in question has the typical pulse shape associated with a positive augmentation

index, which is defined as (height of #2 pulse – height of #1 pulse)/maximum overall amplitude. [24] A positive augmentation index is usually taken to be indicative of arterial aging, which, given the subject’s age, is unlikely to be the case. This subject’s pulse shape returned, along with normalizing systole, within minutes to the original line shape (top trace in Figure 2B).

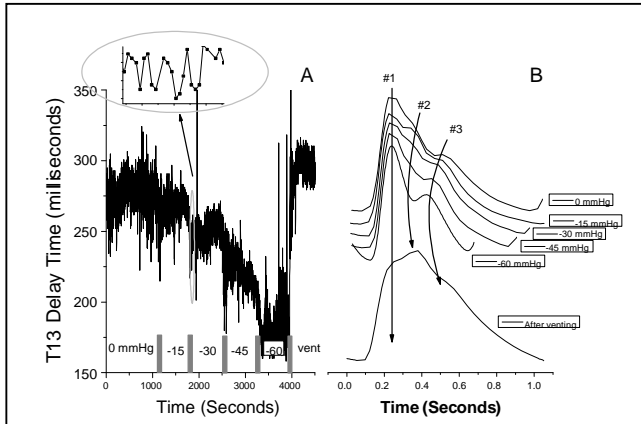


Figure 2: Evolution of T13 parameter (graph A) and corresponding arterial pressure pulse line shapes (10-pulse averages) for subject #5, 31 y. f., over the course of an entire LBNP session. The narrowing of the arterial pulse is indicated by the downward (with time) pointing arrows that identify the changing temporal position of component pulses #2 and #3 relative to the primary systolic pulse #1. In this subject the heart rate changed significantly. Note the different rate of change in the T13 interval and the heart rate. Of interest also is the massive rebound that is observed in the #2 component pulse amplitude after venting, which subsided within minutes.

While the results displayed in Figure 2 exhibited a significant change in heart rate along with the change in T13, this was not a general observation. **Figure 3** presents the results regarding inter-beat interval and T13 for subject #9, a 24 y. male, who did

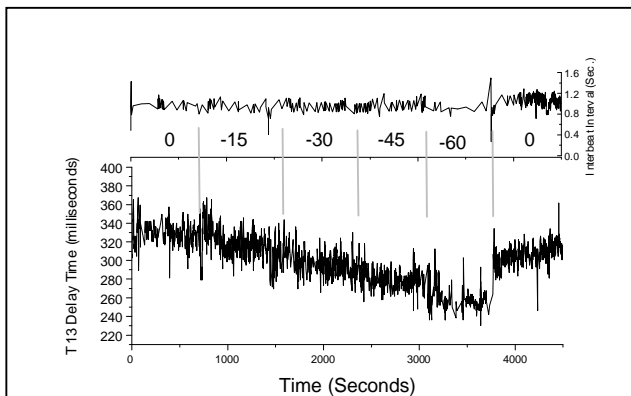


Figure 3: Temporal evolution of the inter-beat interval and T13 over the course of the LBNP session of subject #9, 24 y. m.. In this subject the narrowing of T13 was observed without any change in heart rate until venting.

not exhibit any appreciable change in heart rate until venting. The narrowing of T13 with decreasing negative pressure, however, matched those of all the other subjects.

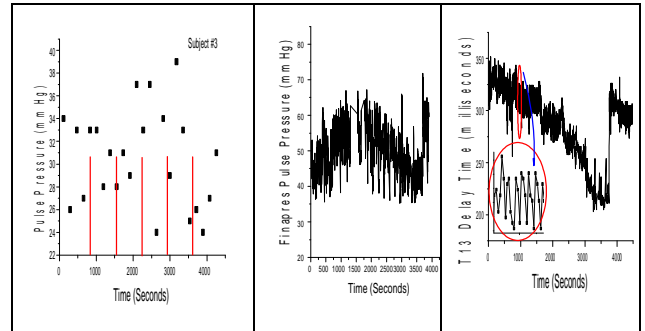


Figure 4: Comparison of the individual results for cuff-based pulse pressure (left graph), Finapres-based pulse pressure (center), and PDA-based T13 measurements, for subject #3. The right panels present the simultaneously obtained T13 delay times between the primary left-ventricular ejection pulse and the iliac reflection pulse recorded on the subject’s middle member of the middle digit.

Figure 4 displays a representative side-by-side comparison of pulse pressures obtained with the automatic cuff (left graph) and the Finapres (center graph), as well as the evolution of the T13 parameter over the course of the LBNP session of subject #3, (right graph). The general absence of a discernible trend in the readings of the cuff with progressing hypovolemia was typical for all data runs.

Figure 5 presents comparative overall results for pulse pressures and T13 as a function of progressive decreasing negative pressure. Specifically, Figure 5A presents the overall pulse pressure results of the automatic pressure cuff while Figure 5B presents the overall results for T13. Figure 5C presents overall pulse pressure results for the Finapres.

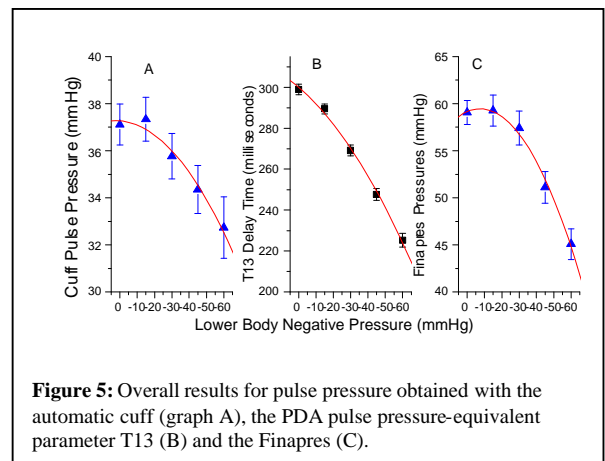


Figure 5: Overall results for pulse pressure obtained with the automatic cuff (graph A), the PDA pulse pressure-equivalent parameter T13 (B) and the Finapres (C).

The ability of the three measurement methods to resolve the effects of the different LBNP stages at a statistically significant level varied. While the PDA method was able to resolve each of the four LBNP stages relative to atmospheric pressure, neither the Finapres nor the cuff were able to resolve the stages with the two least negative pressures (-15 & -30 mmHg), corresponding to the smallest changes in pulse pressure, with significance set at $p \leq 0.05$. Table 1 presents the results of the ANOVA analysis.

Of interest also is the degree to which the PDA parameter T13 correlates with arterial pulse pressure. The parameter correlated

linearly with the pulse pressure determined using the Finapres and the cuff at a statistically significant level ($0.19 \times T13$ (milliseconds) + 2.58, $R^2 = 0.98$, $p < 0.0001$).

Table 1:
ANOVA: PDA, Finapres, Cuff versus
LBNP (-15 & -30 mmHg)

Factor	Type	Levels	Values
LBNP	fixed	2	1, 2

Analysis of Variance for PDA

Source	DF	SS	MS	F	P
LBNP	1	1113.8	1113.8	48.32	0.0001
Error	92	2120.7	23.1		
Total	93	3234.6			

S = 4.80119 R-Sq = 34.44% R-Sq(adj) = 33.72%

Analysis of Variance for Finapres

Source	DF	SS	MS	F	P
LBNP	1	60.3	60.3	0.23	0.636
Error	92	24540.0	266.7		
Total	93	24600.3			

S = 16.3321 R-Sq = 0.25% R-Sq(adj) = 0.00%

Analysis of Variance for Cuff

Source	DF	SS	MS	F	P
LBNP	1	403.8	403.8	1.57	0.214
Error	92	23688.4	257.5		
Total	93	24092.2			

S = 16.0463 R-Sq = 1.68% R-Sq(adj) = 0.61%

IV. DISCUSSION

The results presented support the hypothesis that the time delay between the primary component pulse (#1) and the iliac reflection pulse (#3), T13, correlates with pulse pressure. Clearly of interest now is to provide a physiological and quantitative model that can explain the origin of the observed correlation.

A The PDA model

The hypothesis of two distinct central pressure pulse reflection sites makes it possible to propose a simple model of the arterial paths that the primary pulse and its reflections traverse and to compare its predictions with observations regarding the relative arrival times of the different component pulses. The model's equations predict the time of arrival of each individual component pulse, subject to the total distance that the pulse has traveled and the *pressure-dependent* pulse propagation velocity in each arterial segment. The different relevant arterial paths are denoted by x_n , where x_1 refers to the arm arterial path while x_2 , x_3 refer to the thoracic and abdominal aorta, respectively. t_n refers to the time of arrival of the nth component pulse at the radial/digital arterial peripheral site. While in the case of the #1 pulse its arrival time, t_1 , is determined only by its travel along the arm complex arteries (x_1 path), the arrival times for the #2 and #3 pulses take into account their initial travel as the primary ejection pressure pulse as well as, after impacting a reflection site, their subsequent return as a reflected pulse. As an example, the "second systolic" (#2) pulse traverses the thoracic aorta at systolic pressure, traverses it again as an R2 reflection after re-direction at the renal arteries reflection site (indicated as R2 of

pulse pressure plus diastolic pressure) and then enters the arm arteries where it loses another percentage of its amplitude due to the R1 reflection coefficient that incorporates artery segment transitions, such as the aortic/subclavian junction.

$$t_1 = \frac{x_1}{v_{arm, systole-R1*PP}}, \quad \text{where} \quad v = \sqrt{\frac{hE_a \xi^2 P}{2\rho \alpha}}$$

$$t_2 = \frac{x_2}{v_{aorta, systole}} + \frac{x_2}{v_{aorta, diastole-R2*PP}} + \frac{x_1}{v_{arm, diastole-R2*(1-R1)*PP}}$$

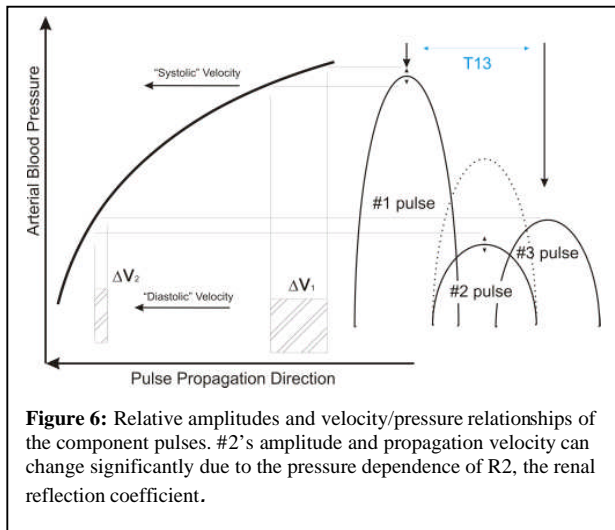
$$t_3 = \frac{x_3}{v_{aorta2, systole-R2*PP}} + \frac{x_2}{v_{aorta1, systole}} + \frac{x_3}{v_{aorta2, diastole-R3*(1-R2)*PP}} + \frac{x_2}{v_{aorta, diastole-R3*(1-R2)*(1-R2)*PP}} + \frac{x_1}{v_{arm, diastole-R3*(1-R2)*(1-R2)*(1-R1)*PP}}$$

The pressure dependence of the pulse propagation velocity is implemented using the Moens-Korteweg¹⁷ equation relating pressure and velocity. Its definitions are as follows: $v_{x,P}$ is the velocity of the xth arterial pulse path at the pressure P indicated. E is the Young's modulus, α is the artery's diameter, h is the arterial wall thickness, ρ is the fluid density, ξ is the arterial compliance and P is the pressure and PP is the pulse pressure. The Young's modulus and the arterial extensibility ξ are different for the different arterial segments.

Another critical feature of the model is that R2, the renal reflection coefficient, is dependent on systolic pressure. The motivation for this is based on the following consideration. As discussed, the renal reflection (P2 pulse) originates at the junction between thoracic and abdominal aorta, a junction that is characterized by a significant change in arterial diameter. Since the thoracic aorta is the softest artery in the body, and much more extensible than the abdominal aorta, increasing peak pressure, or systole, will enlarge the diameter mismatch, giving rise to a more pronounced renal reflection pulse amplitude while falling systole will produce the opposite effect. The critical insight then is that the amplitude of the renal reflection will increase relative to the amplitude of the primary systolic (P1 pulse) peak because, while both component pulses travel the arteries of the arm complex, and are therefore both subject to the pulse narrowing and heightening due to the taper and wall composition changes of the peripheral arteries, only the renal reflection will have sampled the pressure-induced aortic impedance mismatch changes. This establishes the motivation for taking the ratio of the amplitudes of the #2 and the #1 pulse, which is P2P1.

The pulse pressure line shapes observed after venting qualitatively support the physical description presented above. As we pointed out in the discussion of the line shapes presented in Figure 2, the line shape recorded immediately after venting exhibited a massive second systolic peak (#2) amplitude, simultaneously with which significant increases in systolic pressure were recorded using the conventional blood pressure monitors. After a few minutes and in parallel with a recorded decrease in systolic blood pressure, the amplitude of the second systolic peak (#2) returned to its original amplitude.

A similarly physical argument can be made for the difference in arrival times of the primary pulse (#1) and the iliac reflection (#3), or T13. The difference in the arrival times of the primary arterial pulse, that is the left ventricular ejection, and the iliac reflection pulse is determined by the differential velocities with which both pulses propagated along their arterial paths. In the case of the iliac reflection the path length is longer than that of the primary pulse by almost twice the length of the torso. More importantly, both pulses travel at different velocities because their pressure amplitudes are different. Specifically, the iliac reflection pulse amplitude, which is determined by the reflection



coefficient of the iliac reflection site, is on the order of 40% of pulse pressure. This point is graphically made in Figure 6. Both pulses therefore load the arterial wall differently during their arterial travel, as a result of which their propagation velocities are different. The second insight is that, because the pressure/velocity response curve is non-linear, a result known since the 1960s based on Anliker's work,¹⁸ both pulses accelerate and decelerate at different rates as the pressure rises and falls. The primary pulse experiences the highest changes in velocity as a function of changes in blood pressure because it is subject to the steepest section of the pressure/velocity response curve, while the iliac pulse, "running" at much lower pressure, changes velocity much more gradually. Changes in the time of arrival therefore then reflect changes in the differential arterial pressure that the two pulses experience. While this differential pressure is not exactly pulse pressure, that is the difference between the full pulse arterial pulse height and the diastolic pressure floor, it represents about 60%-70% of it, assuming the previously stated iliac reflection coefficient.

Figure 6 presents a graphic display of the relative amplitudes of the left ventricular ejection (#1) and the trailing reflection pulses and their resulting relative positions on the pulse propagation velocity curve, which is highly pressure dependent. As a result the arrival times of the different pulses are highly pressure dependent, a point that is clarified by Figure 7, which presents the pulse travel times, from bottom to top, respectively, of the the primary ejection pulse (#1), the renal reflection (#2), and the iliac reflection (#3). The iliac pulse's arrival time shortens only

slightly with increasing pressure because its amplitude remains close to the diastolic pressure regime. The renal reflection peak's arrival time (middle) experiences significant non-linearity because the reflection coefficient, R2, is highly pressure dependent. The left ventricular ejection (#1, bottom curve) has the highest amplitude and samples the steepest section of the pressure/velocity curve and is therefore most pressure dependent. Using Young's moduli obtained from the literature and letting the model fit R2 as well as the velocities of the primary arterial path ways it is then possible to compare experimental data with model predictions.

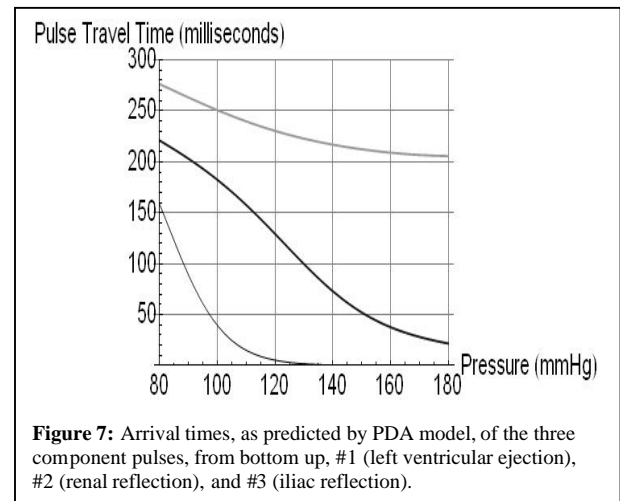
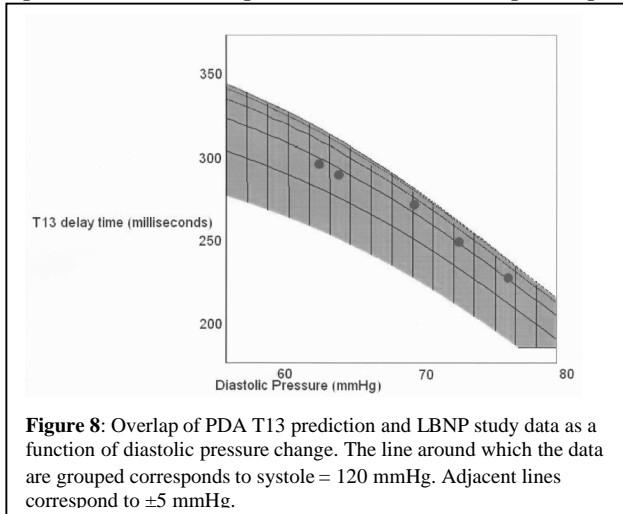


Figure 7 displays the fact that human arterial pathways, for the average height population we have studied, are generally very short relative the distances the arterial pulse traverses within a cardiac cycle. Typical arterial pulse propagation velocities range, for healthy and unstressed arteries, from 4 – 9 m/s. This fact influences particularly the arrival time of the #1 pulse profoundly. In the lower pressure range, which is the pressure regime that was examined here, the #1 pulse pulls away from the #2 and #3 reflection pulses, as evidenced by the fact that its arrival time shortens significantly faster with increasing pressure than the arrival times of #2 and #3. Consequently, in this pressure range, T13 would be expected to widen with increasing pressure and shorten with decreasing pressure. Figure 7 therefore provides a quantitative basis for why T13 is directly dependent on blood pressure changes in the blood pressure regime that was examined here.

As the pressure continues to increase, however, the arrival time of the primary #1 pulse saturates as it runs out of arterial runway. Consequently further increases in arterial pulse propagation velocity do not result in a further shortening of the arrival time. Meanwhile the #3 pulse continues to accelerate with increasing pressure, narrowing the T13 time delay in this high-pressure regime. The details of the pressure-dependent evolution of the arrival time curves are critically dependent on the choice of different velocity profiles for the different arterial sections, a point that is discussed in the following section.

B. Comparison with model predictions

Using the experimental T13 and blood pressure values we compare these with the predictions of the PDA model and explore the relative temporal behavior of the component pulses.



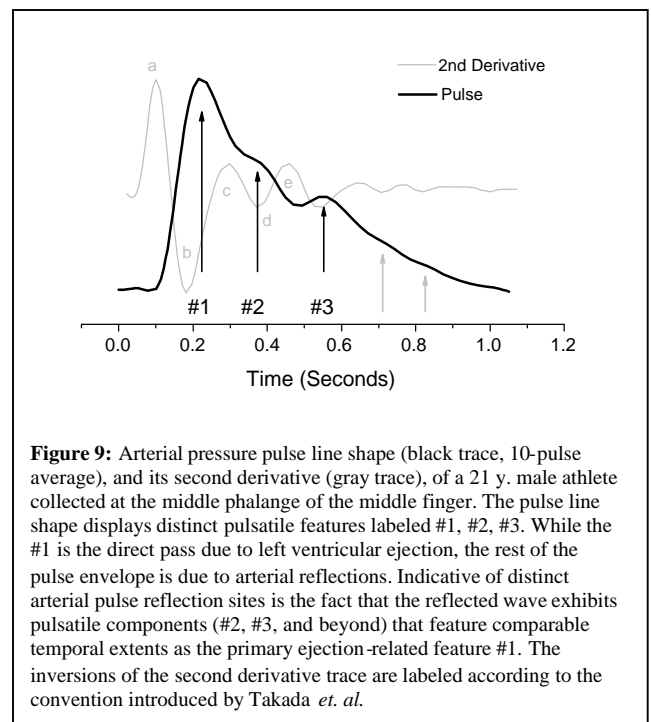
In Figure 8 we present an overlay of the experimental results and the model's predictions. The experimental data, all averages from 15 subjects, are the T13 values obtained from each LBNP stage as well as the corresponding pulse pressure values as determined with the Finapres. Since systole did not change appreciably for any of the subjects, we use the average value of 120 mmHg throughout. Consequently, as observed experimentally, changes in pulse pressure are driven entirely by changes in diastole. The most important aspect of the agreement between the model and data, as presented in Figure 8, are the arterial parameter assumptions that are required to achieve it. The single dominant factor that determines the response of T13 to pressure changes is the pressure/arterial pulse velocity response of the different arterial sections that the systolic pulse and its two central reflections traverse. Furthermore the range of relative pressure/velocity response curves that is possible, given the constraints of the experimental data, is very narrow. Clearly the model at this stage uses a significant simplification of the arterial path sections and the response curves presented represent averages over these pathways. While more details will be introduced in future versions of the model the aim here is to demonstrate that the basic physical picture hypothesized by the PDA model matches observations.

While the starting values of the pressure/velocity curves for the arm complex arteries as well as the thoracic/abdominal aorta were based on published arterial pulse propagation velocities,⁶ the results of the LBNP experiments provide an opportunity to deduce the relative dynamic response characteristics of the different sections, which are not readily available as they have not been the subject of research interests in a long time. In order to obtain the fit shown in Figure 8, a different dynamic behavior of the arm complex relative to that of the central arteries had to be modeled. Specifically, while the arm complex arteries required a distinct exponential response characteristic, the simulated central arteries' response, in the blood pressure range under consideration, was essentially linear. And it is this

difference in dynamic response that enables the model to generate T13 curves whose slopes match those observed. In contrast, changes in starting values only shifted the family of curves in parallel up or down in but did not change the relative slopes of the curves.

C. Other considerations in support of the PDA model

Other considerations further buttress the case for the physical PDA model proposed here. One is that the arterial pressure pulse exhibits distinct features that have the same temporal characteristics as the left ventricular ejection pulse, and these features can be individually manipulated, making the concept of summed reflections from different reflection sites unlikely. Another consideration is that the timing between the ejection pulse and the reflected pulses matches those predicted by the PDA model while being incompatible with the notion that the reflections originate from reflection sites in the distant arterial periphery.



As an example regarding the distinct temporal features of the pressure pulse, Figure 9 displays the 10-pulse average of the arterial digital pressure pulse of a 21 y. male athlete. A very similar line shape, though obtained at the radial artery, is displayed in Millasseau.¹² The pulse displays three distinct features, indicated by the black marked arrows. In order to accentuate their temporal extent, the trace of the second derivative of the pulse is overlaid in light gray color. Presumably, the primary peak (#1) corresponds to the left ventricular ejection, while the other two peaks are part of the reflected wave. However, why are there two distinct pulses that constitute the reflected wave and why do they have a temporal width comparable to that of the primary wave? If the reflected wave were the summation of many different waves originating

from different reflection sites, the temporal character of the original pulse would wash out in the reflected wave. Put differently, the reflected wave would be expected to display an amorphous character instead of displaying distinct features.

Another important observation is that the pulse-like features in the reflected wave can be independently manipulated. Figure 10 displays a different subject's digital pressure pulse over the course of the onset and until just before the release of a Valsalva maneuver. The temporal progression from one pulse to the next is in a downward direction in the figure. The change in contour is unmistakable in that the #2 component pulse progressively diminishes in amplitude relative to the primary pulse (#1) and *relative to the second reflected pulse (#3)*. If, as suggested by the current view, the reflected pressure pulse wave is a summation of reflections returning from various parts of the arterial periphery, why is a maneuver that manipulates pressure within the thorax able to modify a part of it more strongly than another part? The fact that the #2 pulse can be directly manipulated through valsalva strongly suggests that this reflection indeed originates from a reflection site within the thorax.

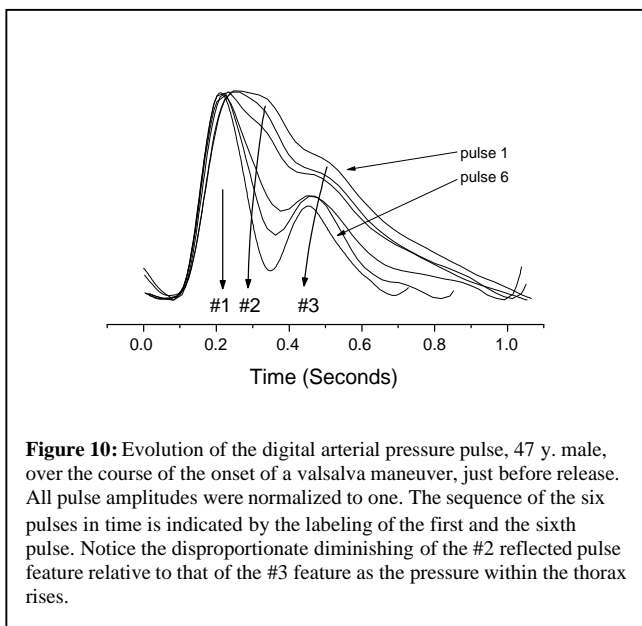


Figure 10: Evolution of the digital arterial pressure pulse, 47 y. male, over the course of the onset of a valsalva maneuver, just before release. All pulse amplitudes were normalized to one. The sequence of the six pulses in time is indicated by the labeling of the first and the sixth pulse. Notice the disproportionate diminishing of the #2 reflected pulse feature relative to that of the #3 feature as the pressure within the thorax rises.

Another objection to the current view is that the timing of the trailing reflected pulse relative to the primary systolic pulse is simply not compatible with the concept of them having returned from distant arterial reflection sites. As an example, the #2 pulse of Figure 9 typically appears between 70-140 milliseconds after the primary ejection⁶ at a pulsation site such as the radial artery or the finger. In order for this peak to have originated in the distant arterial periphery of the “lower body” and to appear on the order of 100 milliseconds past the primary (#1) pulse at the radial artery, its velocity would have had to approach an unreasonable 20 m/s, assuming an arterial pulse path of about 2 meters; from the left ventricle to the upper part of the legs, back through the length of the torso, and along the length of the arm.

Simple considerations also establish that the #2 pulse cannot be traveling in the opposite direction of the primary pulse, as suggested by the current view. If so, it would be a reflection from reflection sites in the hand of the monitored limb. At accepted arterial pressure pulse propagation velocities of about 7 m/s second in the radial artery, such a reflection would appear within a few milliseconds after the primary wave because the arterial pathway to the hand and back is on the order of a few centimeters. Also, the fact that essentially the same time separation between #1 and #2 peak is observed both at the radial artery and the digits further establishes that 1. the #2 peak does not originate in the arm complex arteries, a point made by Millasseau¹² concerning the reflected wave in general, and 2. *it travels in the same direction as the primary #1 pulse.*

The reflection site at the height of the renal arteries was measured directly by Latham,¹⁹ who performed a detailed experimental study to map out the shape of the pressure pulse in the different sections of the aorta simultaneously using a catheter with seven spaced micromanometers. At the junction between thoracic and abdominal arteries, close to the location of the renal arteries, the diameter of the aorta, which tapers continuously away from the heart, undergoes its greatest change. This discontinuity between thoracic and abdominal aorta presents a significant impedance mismatch to the traveling pressure pulse, as a result of which an appreciable part of its amplitude, about 17%, is reflected. Latham also demonstrated that the reflection site could be modulated using valsalva. The effect of the maneuver is to increase pressure within the thoracic cavity, as a result of which the thoracic aorta's diameter shrinks relative to the diameter of the abdominal aorta, which is not affected by the maneuver. The impedance mismatch due to unequal arterial diameters is therefore reduced, which reduces the amplitude of the reflected pressure pulse, the #2 pulse.

Similar considerations apply to the iliac reflection, the #3 pulse. This peak typically appears between 180 to 400 milliseconds after the #1 left ventricular ejection pulse. This pulse again displays, like the #2 pulse, a comparable temporal extent as the primary systolic peak (#1) Several points are of interest. 1. Sampled at the radial or digital artery, in which direction is it traveling? If it were traveling in the opposite direction of the primary peak the same argument offered for the direction of travel of the #2 pulse would apply, i.e. it would have had to be reflected from the end of the monitored limb, from which it would return in a few milliseconds. Since this physical picture is irreconcilable with the long time delay between #1 peak and the #3 feature, and the fact that the feature is observed at radial as well as digital arterial observation sites, *it has to be traveling in the same direction as the primary pulse and it did not originate in the arm complex arteries.* 2. Since it arrives after the #2 peak, its reflection site must lie past the renal reflection site. The next major arterial impediment that could give rise to a substantial pressure pulse reflection, assuming healthy arteries, is the iliac bifurcation. Latham's results also determined the existence of such a reflection site in the vicinity of the iliac bifurcation and he demonstrated that the feature can be manipulated. Specifically, bilateral femoral artery occlusion increased the feature's

amplitude, presumably by increasing the reflection coefficient, while the Mueller maneuver decreased it. Also, timing considerations again support the choice of the iliac reflection site. Assuming an arterial pathway of about 2 meters, the #3 pulse, appearing about 300 ms behind the primary peak, would have traveled at an average arterial pressure pulse velocity of 6.6 m/s, an entirely reasonable estimate.

In more recent work, all the central arterial pulse reflections were mapped out by J. Kriz *et al.*²⁰, who showed that it is possible to use force plate measurements as a noninvasive method to perform ballistocardiography, which is the motion of the body associated with heart activity and pulse propagation. Interestingly, in addition to the reflected pulses originating from the renal and iliac reflection sites his very sensitive setup also determined the existence of harmonic reflection pulses that arrive even further in time, but at the time intervals identical to the time interval between the #2 (renal) and #3 (iliac) pulses. These pulses are re-reflections off the two reflection sites that are, as secondary reflections, very weak in amplitude, making them difficult to observe in the arterial periphery. In Figure 9 the light gray arrows indicate their possible temporal position.

D. Implications of the PDA model

An important point to realize is that any reflection sites in the arm complex arteries do not affect to the pulse line shape that is observed at the radial/digital arteries because any pulse reflections due to such reflection sites will travel *away* from the radial/digital pulsation site and back toward the central arteries. Their re-entry into the arm complex arteries could only be accomplished as re-reflections, with dramatically reduced amplitudes that would be masked by the primary renal and iliac reflections.

Another important point is that the head plays a *much diminished role* in regard to pressure pulse reflections that are observed at the arterial periphery of the arm. Arterial pressure pulse reflections that return via the carotid arteries will, upon entering the aortic arch and traveling along the descending thoracic, re-reflect off the reflection site in the vicinity of the renal arteries. Assuming a reflection coefficient on the order of 17%, the amplitude of such a re-reflection will be on the order of 3% of the primary peak amplitude, and consequently be again masked by the much larger pressure primary pulse reflections #2 and #3.

The PDA model also ties together recent related observations by others. The fact that the ratio of the amplitudes of the #2 (P2) and #1 (P1) pulses correlates with systolic pressure is not surprising in light of the results obtained by Takazawa *et al.*,²¹ Takada *et al.*,²² and Imanaga *et al.*²³ In **Figure 9** we also presented the second derivative of the arterial pulse. Takazawa *et al.* labeled the different inversions, called “waves”, of this second derivative trace as indicated in the figure. The results of several studies suggest that the ratio d/a correlates with blood pressure, along with many other physiological parameters. [21, 22] Comparative inspection of the two traces establishes that the

waves “a” and “d” are temporally in very similar positions to P1 and P2, respectively. A parameter introduced by Bartolotto²⁴ that incorporates *very similar definitions* of P1 and P2 as the PDA model was also found to correlate with systolic pressure. This parameter is the augmentation index of the photoplethysmograph, PTG (AUGI), and it is defined as $(P2 - P1)/MA$, where P2 and P1 are the amplitudes of the primary and second systolic peaks in the photoplethysmograph, respectively, and MA is the maximum envelope amplitude. These correlative results support the PDA model, which supplies the physical explanation both for the origin of the component pulses as well as why the correlation of the relative amplitudes of these component pulses with systolic pressure exists.

As with the PDA’s P2P1 parameter, others have suggested measures that utilize the same time interval corresponding to T13 and have somewhat comparable physical interpretations. Millasseau [12] labels the time delay PPT in the digital volume pulse and suggests that it corresponds to the transit time of pressure waves from the root of the subclavian artery to the “apparent” site of reflection “in the lower body” and back to the subclavian artery. The reason for choosing the subclavian artery as a starting and ending point is however unclear, since the pressure wave does not originate there. If, on the other hand, the subclavian artery were to give rise to the #3 pressure pulse as a reflection site, the amplitude of the iliac pulse would dramatically lower than what is observed (20-40% of the primary peak) at the radial or digital artery. Succinctly put, the pulse would have traveled from the left ventricle to the subclavian artery, reflected there at some reflection site, then to travel to the iliac reflection site. It would return from there as a re-reflection pulse with commensurately much reduced amplitude, an unlikely scenario.

A significant benefit of measuring T13 over pulse pressure directly is its higher resolution and sensitivity. The results indicate the equivalence of a change of about 200 milliseconds in T13 to a variation of about 8 mmHg in pulse pressure *over the entire range* of a simulated central blood loss in excess of 1 liter for this cohort of fit and relatively young subjects. The results therefore indicate that the PDA technology is capable of resolving small changes in pulse pressure, a feat that sphygmomanometers are not well suited for. Given the suggestion by others that pulse pressure can be considered as a surrogate for stroke volume and therefore as a means to track loss of blood volume in trauma patients,⁴ the accurate monitoring of pulse pressure could be a vital component in predicting the onset of hemorrhagic shock.

The potential benefits of utilizing T13 in detecting small changes in pulse pressure, coupled with the small size of the CareTaker hardware, which weighs on the order of 5 oz, and the fact that it tracks blood pressure at low coupling pressures, makes the system attractive for the monitoring of patients at risk for internal hemorrhage. A benefit of such field-based monitoring is that internal hemorrhage could be detected well before hemodynamic collapse, making timely intervention feasible.

A limitation of this study is that it was conducted under ideal condition, whereas mobile settings are likely to introduce movement artifacts. Tests are planned to examine the performance of the CareTaker system in emergency vehicles.

Conclusions

We have presented a new physical model of the propagation of the arterial pressure pulse and its reflections as well as a comparison of the predictions of the model with experimentally obtained pulse parameters and conventionally obtained blood pressures. The agreement of observations and measurements provides a preliminary validation of the model which in turn could provide a renewed impetus in the study of the human arterial pressure pulse. The model is based on few, physical, assumptions because it proposes that the structure of the pulse is due to it is readily identifiably arterial pulse reflection sites. As a result it is also readily testable.

¹ Bellamy RF. The causes of death in conventional land warfare: implications for combat casualty care research. *Mil Med.* 1984;149:55–62.

² Carrico CJ, Holcomb JB, Chaudry IH, PULSE trauma work group. Post resuscitative and initial utility of life saving efforts. Scientific priorities and strategic planning for resuscitation research and life saving therapy following traumatic injury: report of the PULSE trauma work group. *Acad Emerg Med.* 2002;9:621–626.

³ Convertino VA, Cooke WH, Holcomb JB. Arterial pulse pressure and its association with reduced stroke volume during progressive central hypovolemia. *J Trauma.* 2006 Sep;61(3):629–34.

⁴ Leonetti P, Audat F, Girard A, Laude D, Lefrere F, Elghozi JL. Stroke volume monitored by modeling flow from finger arterial pressure waves mirrors blood volume withdrawn by phlebotomy. *Clin Auton Res.* 2004;14:176–181.

⁵ Davis, JJ, Band MM, et. al, Peripheral blood pressure measurement is as good as applanation tonometry at predicting ascending aortic blood pressure. *J. of Hyperten.* 2003, 21:571–576.

⁶ Nichols WW, O'Rourke MF. McDonald's blood flow in arteries. Theoretical, experimental and clinical principles. London: Edward Arnold;1999.

⁷ Soderstrom S, Nyberg G, Ponten J, Sellgren J, O'Rourke MF. Substantial equivalence between ascending aortic pressure waveforms and waveforms derived from radial pulse using a generalised transfer function? [Abstract]. *FASEB J* 1998; 12:4131.

⁸ Mitul Vyas, et. al, Augmentation Index and Central Aortic Stiffness in middle-aged to elderly individuals. *Am J Hypertens* (2007) 20:642–647

⁹ London GM, Blacher J., Pannier B, Guerin AP, Marchais SJ, Safar ME, Arterial wave reflections and survival in end-stage renal failure. *Hypertension*, 2001;38:434–438.

¹⁰ Karamanoglu M, Gallagher DE, Avolio AP, O'Rourke MF, Functional origin of reflected pressure waves in a multibranch model of the human arterial system. *Am. J. Physiol* 267 (Heart Circ. Physiol. 36): H1681–H1688, 1994.

¹¹ Bryan Williams, Pulse wave analysis and hypertension: evangelism versus skepticism. *J Hypertension* 2004, 22:447–449.

¹² Millasseau SC, Ritter JM, Takazawa K, Chowienczyk PJ, Contour analysis of the photoplethysmographic pulse measured at the finger. *J. Hypertens* 2006, 24:1449–1456.

¹³ Avolio AP, et. al, Role of Pulse Pressure Amplification in Arterial Hypertension. *Hypertension*, 2009;54:375–383.

¹⁴ Pauca AL, Kon ND, O'Rourke MF. The second peak of the radial artery pressure wave represents aortic systolic pressure in hypertensive subjects. *Br J Anaesth.* 2004;92:651–657.

¹⁵ Cooke WH, Salinas J, Convertino VA, et al. Heart rate variability and its association with mortality in pre-hospital trauma patients. *J Trauma.* 2006;60:363–70; discussion 370.

¹⁶ Cooke, William H, and Convertino, Victor A, Heart Rate Variability and Spontaneous Baroreflex Sequences: Implications for Autonomic Monitoring During Hemorrhage. *J. Trauma, Injury, Infection, and Critical Care*, 58(4):798–805, April 2005.

¹⁷ Korteweg DJ. Ueber die Fortpflanzungsgeschwindigkeit des Schalles in elastischen Rohren. *Annals Phys Chem (NS)* 1878; 5:520–537.

¹⁸ Anliker M, Histan MB, Ogden E, Dispersion and Attenuation of Small Artificial Pressure Waves in the Canine Aorta. *Circ. Res.* 1968;23:539–551

¹⁹ Latham, RD et. al, Regional wave travel and reflections along the human aorta: a study with six simultaneous micromanometric pressures. *Circulation* 72, 1985, 1257–69.

²⁰ Kriz J. et al, Force plate measurement of human hemodynamics, *Nonlinear Biomed Phys.* 2008 Feb 22;2(1):1

²¹ Takazawa K, Tanaka N, Fujita M, Matsuoka O, Saiki T, Aikawa M, et al. Assessment of vasoactive agents and vascular aging by second derivative of the photoplethysmograph waveform. *Hypertension* 1998; 32:365–370.

²² Takada H, Washino K, Harrell JS, Iwata H. Acceleration plethysmography to evaluate aging effect in cardiovascular system. *Med Progress Technol* 1997; 21:205–210.

²³ Imanaga I, Hara H, Koyanagi S, Tanaka K. Correlation between wave components of the second derivative of plethysmogram and arterial distensibility. *Jpn Heart J* 1998; 39:775–784.

²⁴ Bortolotto LA, Blacher J, Kondo T, Takazawa K, Safar ME. Assessment of vascular aging and atherosclerosis in hypertensive subjects: second derivative of photoplethysmogram versus pulse wave velocity. *Am J Hypertens* 2000; 13:165–171.